

Solar Flare Measurements with STIX and MiSolFA

Diego Casadei

FHNW, School of Engineering, Bahnhofstrasse 6, CH-5210 Windisch, Switzerland.

Abstract—Solar flares are the most powerful events in the solar system and the brightest sources of X-rays, often associated with emission of particles reaching the Earth and causing geomagnetic storms, giving problems to communication, airplanes and even black-outs. X-rays emitted by accelerated electrons are the most direct probe of solar flare phenomena. The Micro Solar-Flare Apparatus (MiSolFA) is a proposed compact X-ray detector which will address the two biggest issues in solar flare modeling. Dynamic range limitations prevent simultaneous spectroscopy with a single instrument of all X-ray emitting regions of a flare. In addition, most X-ray observations so far are inconsistent with the high anisotropy predicted by the models usually adopted for solar flares. Operated at the same time as the STIX instrument of the ESA Solar Orbiter mission, at the next solar maximum (2020), they will have the unique opportunity to look at the same flare from two different directions: Solar Orbiter gets very close to the Sun with significant orbital inclination; MiSolFA is in a near-Earth orbit. To solve the cross-calibration problems affecting all previous attempts to combine data from different satellites, MiSolFA will adopt the same photon detectors as STIX, precisely quantifying the anisotropy of the X-ray emission for the first time. By selecting flares whose footpoints (the brightest X-ray sources, at the chromosphere) are occulted by the solar limb for one of the two detectors, the other will be able to study the much fainter coronal emission, obtaining for the first time simultaneous observations of all interesting regions. MiSolFA shall operate on board of a very small satellite, with several launch opportunities, and will rely on moiré imaging techniques.

I. INTRODUCTION

SOLAR flares are the most powerful events in the solar system, releasing 10^{25} – 10^{26} J in few minutes [1]. A large fraction of this energy, initially stored in magnetic fields in the solar corona, goes into the acceleration of electrons and ions. Coronal mass ejections (CMEs), often associated with solar flares, may reach the Earth, produce geomagnetic storms, and cause severe problems to communication, airplanes and, in special cases, even large-scale black-outs.

The details of the mechanisms transforming magnetic into kinetic energy are not yet understood. The hard X-rays (HXR) emitted by electrons accelerated during a flare are the most direct probe of the physical processes at the Sun. The brightest X-ray sites are the footpoints of magnetic loops which connect the acceleration regions (higher in the corona; Fig. 1) with the much denser chromosphere, where the electrons interacting with the ambient ions emit bremsstrahlung photons, losing most of their energy. From the measured photon spectrum, one can infer the distribution of the parent electrons, typically a superposition of a thermal component with a non-thermal distribution extending to higher energies. Because the Earth

atmosphere absorbs X-rays, the measurements need to be carried out in space.

The most sensitive solar HXR observatory to date is the Reuven Ramaty High Energy Solar Spectroscopic Imager (RHESSI [2]), using 9 rotation modulation collimators and bulk Ge detectors to perform imaging spectroscopy from 3 keV to 17 MeV with angular resolution of few arcseconds [3]. The X-ray energy spectrum from a solar flare typically shows a thermal component and a non-thermal tail extending possibly to very high energies (Fig. 2). The flux of photons quickly falls down with increasing energy, typically as a power-law with spectral index in the range from 2 to 5 units for the footpoints, and from 3 to 8 for the coronal source [4].

Thanks to RHESSI measurements, it was discovered that 10–50% of the energy release goes into accelerating electrons [5], and that a coronal non-thermal component is present in essentially all flares [6]. Double coronal sources suggest acceleration in the corona [7], and rare observations of coronal acceleration sites suggest energization of practically the entire pre-existing electron population [8]. Hence understanding the dynamics of a solar flare requires measurements of the photon spectra emitted by the top-of-the-loop region together with the footpoints.

During the next solar maximum (beyond the end of the RHESSI mission), the Spectrometer/Telescope for Imaging X-rays (STIX) instrument [9] of the ESA M-class Solar Orbiter mission [10] will allow the scientific community to continue studying the X-ray emission from solar flares with similar imaging spectroscopy performance as RHESSI, although in a smaller energy range (up to 150 keV). Onboard the Solar Orbiter, additional instruments will perform in-situ measurements of solar wind, energetic particles, magnetic field and radio and plasma waves, while others perform remote measurements in different wavelengths, from optical to EUV. Its orbit will pass closer to the Sun than Mercury (with 0.28 AU closest perihelion), allowing STIX to observe it from a wide range in latitude (with 25 deg orbit inclination). STIX exploits the moiré patterns produced by 30 pairs of grids with different periods and relative angle, in order to provide good image quality without a rotating satellite.

Despite from the excellent performance of RHESSI and STIX, solar flares are challenging objects of study for any single HXR instrument. For this reason, we have proposed to build a small detector called MiSolFA (the Micro Solar-Flare Apparatus), orbiting the Earth during the next solar maximum, which together with STIX will obtain qualitatively new information about solar flares. Together, STIX and MiSolFA will be able to address the two main open issues about solar flares, performing a simultaneous measurement of coronal sources and footpoints, and evaluating the X-ray emission as a function

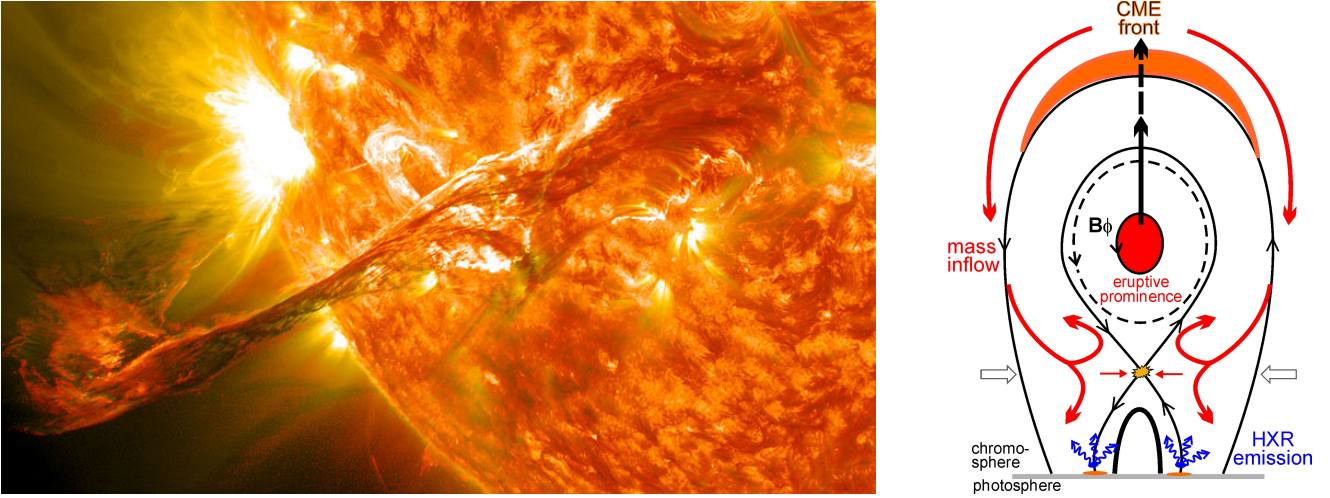


Fig. 1. Solar flare with CME on 2012-08-31 15:22UTC (left) and illustration of a flare and the associated CME (right).

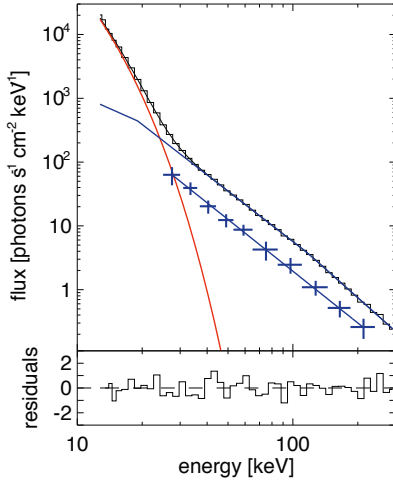


Fig. 2. The RHESSI measurement of the overall spectrum from the bright (X6.5) flare 2006-12-06 18:47UTC shows a thermal (red) and non-thermal (blue; broken power-law) component. The points with error bars are the spectrum from the main footpoint, with a single power-law fit [11].

of the direction and energy.

II. OPEN ISSUES

Because the bremsstrahlung intensity is proportional to the ambient plasma density, the coronal sources (where the acceleration is thought to occur) are 1–2 orders of magnitude fainter than the bright chromospheric footpoints of flare loops (where the electrons loose most of their energy). The indirect imaging technique based on the shadows projected by absorbing gratings on the detector, adopted both by RHESSI and STIX (albeit with different methods), has limitations in dynamic range: a coronal source is practically invisible when a footpoint is inside the field of view of the instrument. Although grazing incidence optics do not have these dynamic range limitations, they can not cover the highest energy range and require very long satellites (the focal distance being of order 10 m), resulting in much higher mission costs. At present, no

dedicated mission is foreseen with these optics for solar flare studies.

So far, the best results have been obtained by studying the solar flares occurring just behind the solar limb, with occulted footpoints but unobscured coronal sources (a few per month during a solar maximum). Statistical studies of partially occulted flares have shown that nearly all contain non-thermal coronal sources [4], but so far the simultaneous observation of footpoints and coronal sources was not possible for any solar flare with the same technique (there were observations from different satellites [12], [13], but systematic effects made it impossible to properly cross-correlate them).

Another problem in understanding solar flares is that most acceleration models produce strongly beamed non-thermal electron fluxes, resulting in highly non-uniform patterns of photon emission. However, there is still no conclusive proof that the emitted photon spectrum is not uniform. So far, HXR directivity has been studied with the following techniques:

- statistical studies of center-to-limb variations in flux or spectral index [14], [15]
- analysis of contributions from reflected radiation in a single flare [16]
- simultaneous observations with different satellites [12], [13]
- polarization measurements with a single satellite [17].

Many, although not all, these studies have found results consistent with an isotropic electron distribution, inconsistent with the strong beaming predicted in the thick-target model used to model the footpoint emission. Thus either we lack good observations or we fail to understand the fundamental theory. The only way of solving this issue is to directly measure the HXR directivity with cross-calibrated detectors observing the same flare from different directions.

Thus, the best option is to have the same kind of instruments observing a solar flare from different points of view. This way, the energy response will be the same, which is a crucial requirement. Indeed, the photon spectrum is so steep that a small change in the measured energy makes a big impact on the overall slope. On the other hand, cross-calibrated instruments

are able to measure the ratio between the intensities along different lines in each energy bin, providing for the first time strong constraints on the emission models. For this reason, MiSolFA adopts the same photon detectors as STIX: the instrument consists of an array of Caliste SO units equipped with CdTe crystals [18]. For the solar flares whose footpoints are occulted by the solar limb for MiSolFA but visible by STIX (or vice versa) it will be possible to measure the energy spectrum of the photons coming from both the corona and the chromosphere. In addition, the emissivity of a source visible by both instruments will be estimated along two different directions as a function of the photon energy.

III. THE MISOLFA DETECTOR

The main scientific goals of the MiSolFA project, ranked by importance, are:

- 1) providing together with STIX simultaneous observations of HXR from coronal and footpoint sources with cross-calibrated detectors, for the first time;
- 2) unambiguously measure for the first time the directivity of HXR emission together with STIX;
- 3) extend the sample of solar flare data with stand-alone observations, when STIX is outside its science windows or it is on the other side of the Sun.

For the subset of CMEs reaching the Earth and detected by MiSolFA, it will also possible to perform a detailed study of the magnetic connectivity from the Sun to the Earth (one of the 4 top-level scientific goals of the Solar Orbiter [10]).

There are two possible configurations, one which shall fully achieve all science goals, and a fallback design which is technically less challenging while preserving most of the science. In the default configuration, X-ray imaging will be indirectly performed along the same lines as STIX, although with less details. This is achieved by placing two opaque grids in front of each Caliste unit, producing moiré patterns whenever a source not much larger than their angular scale (half of the ratio between the grid distance and the grating period) is visible. The fallback configuration omits the grids and, possibly, reduces the number of Caliste units. This implies a reduction in the number of useful flares for the first two science goals, but does not preclude their successful achievement, as even a single well-observed event would be sufficient to perform a significant step forward in our understanding of solar flares. The biggest impact is on the third goal, as imaging adds qualitatively important information to flares observed by MiSolFA alone (for example, it allows for a direct estimation of the source volume). Still, when no other instrument can detect the same event, even the overall spectrum alone brings important information. In the following, only the full configuration is illustrated.

Imaging is performed indirectly: in front of each Caliste unit, two opaque grids will project shadows forming a moiré pattern, whose period matches the detector size and runs along its pixels. The amplitude of each moiré pattern depends on the source size, while the phase depends on the source direction. Hence each pair of grids forms a subcollimator providing information along one direction (orthogonal to the slits) with

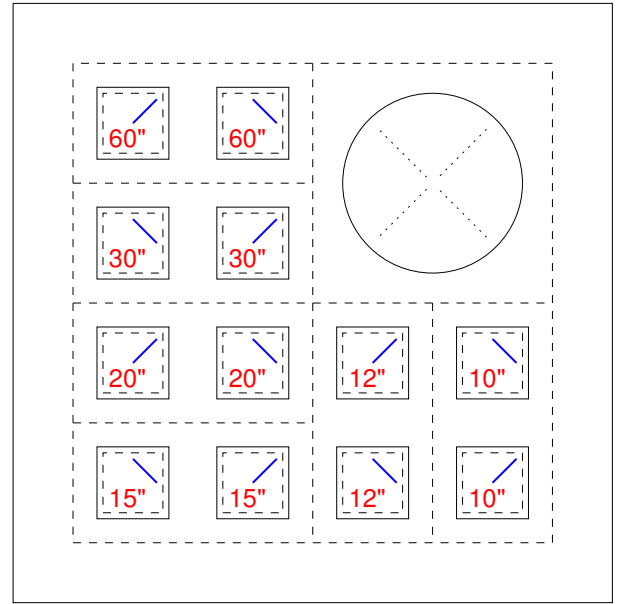


Fig. 3. Layout of MiSolFA detectors, viewed from the Sun.

angular resolution given by (half of) the ratio between the grating period and the separation between front and rear grids.

While for RHESSI and STIX a driver in the design was the ability to span a wide range of angular scales—before RHESSI they were poorly known; STIX will operate in a wide range of distances from the Sun—, this is not an important requirement for MiSolFA. Hence it was preferred to give priority to the image resolution at the expense of the range of angular scales. The first requirement is to separate the footpoints, which translates into a smallest angular scale of about 10 arcseconds. On the opposite side, one wishes to be able to recognize the overall topology of the HXR emission, which means that the detector should cover an angular scale of at least 60 arcseconds. The best image resolution is then achieved by sampling over integer multiples of the baseline angular frequency, as this produces the first terms of a Fourier series. For this reason, the angular scales are chosen equal to $60''/n$ with $n = 1, 2, \dots, 6$.

Next, as it is easier to keep the pointing to the required stability (within 1 degree) when the satellite is not rotating, one should take care of sampling two orthogonal directions at each angular scale. This means that the total number of subcollimators is 12, as shown in Fig. 3. As the slit-to-period ratio is 0.5, the overall transmission is 0.25 at low energy (increasing toward 100% at high energies, when the grids are no more opaque), giving 3 cm² effective area for the thermal component (representing the bulk of the flare emission).

Figure 4 shows the point spread function (PSF) of MiSolFA, which corresponds to the reconstructed image of a simulated point source at the center of the field of view, using two algorithms: backprojection and clean [3]. The backprojected image is obtained by summing, for each photon, its arrival probability distribution. The photon is detected by one of the detectors, which means that it had to cross the two grids in front of it. At low energy, when the grids can be considered

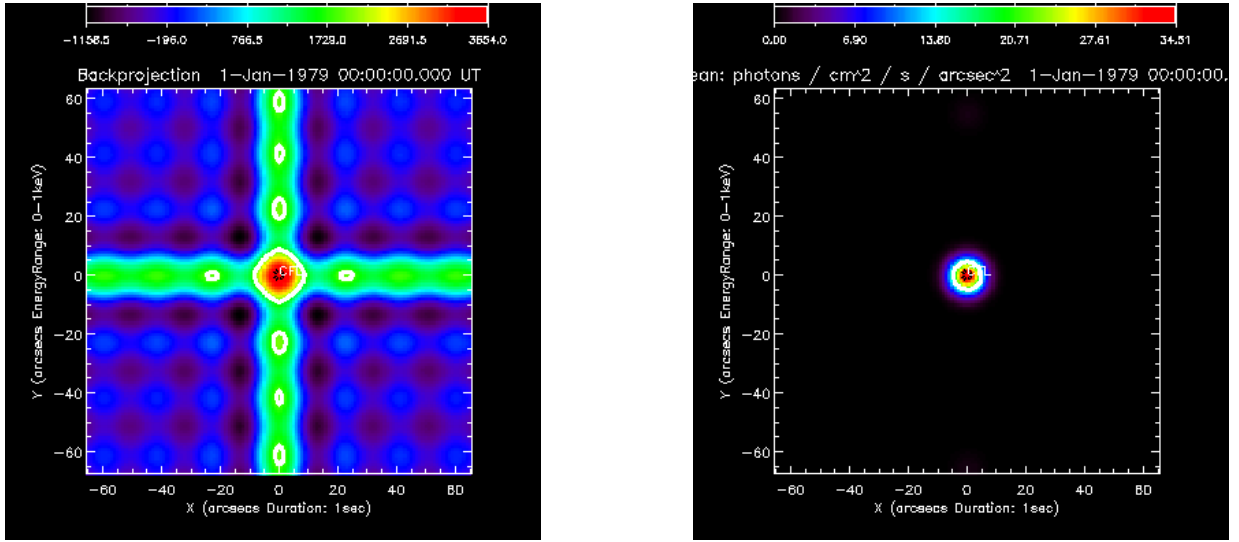


Fig. 4. Point spread function of MiSolFA, with the backprojection (left) and clean (right) algorithms.

opaque, this probability distribution is a collection of excluded areas mimicing the “shadow” of the two grids, intermixed with areas with non-null and uniform probability (neglecting diffraction effects). At energies for which the transparency of the grids is sizable, the “shadow” corresponds to areas with small but not null probability. By summing over the probability distributions of the photons detected by all subcollimators, one gets the position of the source, with a typical spread which has a cross shape. These beams may be removed using the clean algorithm, which starts from the backprojected image and refines it iteratively, by removing the brightest spot and recomputing the image at each step. At the end of the loop, all spots are then summed together, producing an image which is free from the “noise” visible with the backprojection.

MiSolFA images are actually periodic structures: they repeat every 120 arcseconds, as the largest angular scale is $60''$. Hence MiSolFA has to rely on some other observation to provide the precise location of the flare in the field of view (which contains the full solar disc). This compromise is not a real problem, as there are many ways of obtaining this position using data from other observatories. To uniquely identify the position of the flare would require adding angular scales up to about thousand arcseconds (similar to STIX), which can not be achieved in a very small volume. Thus, priority was given to the image resolution at the price of some unimportant ambiguity in the exact location.

The precise position of the Sun inside the field of view of the instrument is provided by an Aspect System (visible at the top-right corner in Fig. 3) derived from STIX: a lens focusing the image of the Sun onto a plate with apertures of different area, viewed by photodiodes. Each of the 4 radial sequences of apertures is viewed by a single photodiode. Their area increases in log-uniform way when moving out from the center of the field of view. When the Sun image moves on the focal plane, it illuminates a variable number of apertures, causing the total intensity measured by each diode to change in steps which also follow a log-uniform scale. This keeps resolution

in pace with the dynamic range, and allows to follow the jitter of the optical axis as a function of time within few arcseconds.

The choice of similar subsystems for the photon detection and the determination of the Sun position, in addition to guarantee cross-calibration, is also a way of insure the space qualification of all critical components, of exploiting the close collaboration of several STIX members, and of reducing the development time. The synergies between the two projects are a very valuable resource. Indeed, the MiSolFA collaboration presently includes the STIX teams in Switzerland (FHNW Windisch and PSI), France (CEA Saclay) and Italy (University of Genova).

Assuming that there is space enough for a 20 cm separation between the grids, the period of all grids is fixed by the series of angular scales mentioned before. The smallest period in MiSolFA is about 20 microns (for $10''$), beyond the current state of the art of grid fabrication for space applications (based on chemical etching of tungsten guided by lithography). Hence it is planned to adopt a different fabrication technique, which shall be finally able to create gold structures as small as 1–2 microns (20–40 times smaller than with chemical etching). The PSI group and microworks in Karlsruhe, Germany, are currently trying to create gratings for phase-contrast radiography [19] and are willing to produce the grids for MiSolFA.

IV. THE SATELLITE

MiSolFA is a very compact detector, with mass around 1 kg, about 3 dm^3 volume, and requiring less than 10 W. Thus, it can be installed on a small micro-satellite. There are few possible options for the platform, although not all can accomodate the full configuration. The preferred option is a 6-units satellite (Fig. 5) jointly developed by Clyde Space in Glasgow, Scotland and the Swiss Space Center (SSC) in Lausanne. Alternatively, MiSolFA could be installed in the simplified configuration on a 3-units satellite. The 6-units platform can offer enough space for an X-ray imaging spectrometer, to be located inside a volume formed by 3 units

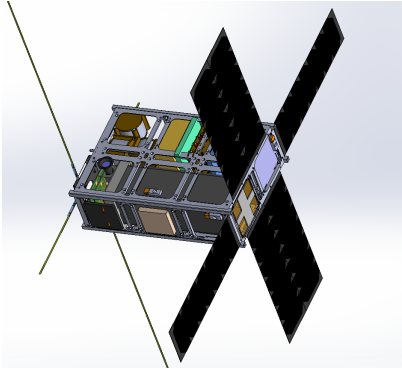


Fig. 5. Preliminary satellite design.

in a row. At the same time it is small enough to guarantee several possibilities for the launch, with an affordable cost. This is essential to guarantee operation during the initial STIX data taking, at the next solar maximum. At the same time, a 6-units satellite can also host two instruments, for example MiSolFA (without imaging) together with another detector. Currently, the most likely candidate is an EUV radiometer developed by PMOD/WRC in Davos, Switzerland.

The main requirement from MiSolFA is a 3-axes stabilized satellite, pointing the Sun and possibly following a Sun-synchronous orbit. The pointing stability should be within 1 deg, well within the capability of commercial attitude control systems. Rather than attempting to improve the stability, the Aspect System is used to provide the precise position of the Sun in the field of view, which allows to correct for the motion of the optical axis during the offline image reconstruction. Pointing to the Sun makes it easy to satisfy the power requirements by means of solar panels. It also provides a quite stable situation from the thermal point of view, as one face is always the hot side and the opposite one is the cold side. The best operating temperature for the Caliste units is -20 C, but the temperature stability is more important than the actual operating point. Preliminary thermal studies indicate that it may be possible to stay within ± 1 C without active cooling if the temperature is not much below 0 C, although work is still in progress on this side.

The onboard data processing shall guarantee the possibility of transmitting to ground entire flares, even in presence of very limited connectivity (9600 b/s for 20 min per day is typical of nanosatellites, and is used as a conservative estimate of the available bandwidth). The simplest approach is to save the information about each individual photon (time, detector, pixel, energy) into a memory buffer. Very large flares may require several hundreds MB, hence a 1 GB buffer shall be adopted. As there are huge differences in photon flux between the thermal and non-thermal regions, it is foreseen to compress the data in a configurable way. Below a certain energy (which may depend on the flare intensity), photons will not be transmitted to ground individually. Rather, histograms will be filled for each detector pixel, representing the photon counts in each energy bin for the considered (configurable) time interval. At higher energies, single photons can be transmitted individually without impacting on the bandwidth requirements.

Finally, to avoid saturation at the lowest energies, a thin layer of absorber (e.g. 0.5 mm Al) will be placed in front of each subcollimator. In addition to provide a light-tight box enclosing the Caliste units, the absorber attenuates in a known way the flux of photons in the soft X-ray range, preventing the saturation of the read-out electronics. No movable attenuator (like in RHESSI and STIX) is foreseen, as its motion would disturb the pointing of the small satellite.

V. SUMMARY AND CONCLUSION

Despite from the great advances in our understanding of solar flares made possible by a dozen years observations by RHESSI, there are still quite a number of open questions. The mechanisms of energy conversion from magnetic to kinetic are not fully understood, nor is the propagation of accelerated electrons in the solar corona. In the next solar maximum period, STIX and MiSolFA will provide simultaneous X-ray observations of solar flares from two different points of view, using cross-calibrated photon detectors. For the first time, it will be possible to measure the faint emission from the acceleration source, at the top of the loop in the corona, together with the much brighter footpoints, at the denser chromosphere. This kind of observation, impossible with a single instrument based on the moiré effect, is necessary to understand the electron acceleration and propagation, the heating of chromospheric plasma and its “evaporation” into the corona. In addition, the directivity of the X-ray emission as a function of the photon energy will be measured, allowing to test the hypothesis of beamed electron transport from the corona down to the chromosphere. This kind of stereo observation will also be able to provide information on the source volume, which is needed when computing the energy budget.

REFERENCES

- [1] A.O. Benz, *Living Reviews in Solar Physics* 5 (2008) 1.
- [2] R.P. Lin et al., *Solar Physics* 210 (2002) 3.
- [3] G.J. Hurford et al., *Solar Physics* 210 (2002) 61.
- [4] S. Krucker & R.P. Lin, *Astrophys. J.* 673 (2008) 1181.
- [5] A.G. Emslie et al., *Astrophys. J.* 759 (2012) 71.
- [6] S. Krucker & R.P. Lin, *Solar Physics* 210 (2002) 229.
- [7] L. Sui & G.D. Holman, *Astrophys. J. Lett.* 596 (2003) L251.
- [8] S. Krucker et al., *Astrophys. J.* 714 (2010) 1108.
- [9] S. Krucker et al., *Nucl. Instrum. Meth. A* 732 (2013) 295.
- [10] D. Müller et al., *Solar Physics* 285 (2013) 25.
- [11] S. Krucker et al., *Astrophys. J.* 739 (2011) 96.
- [12] J.M. McTiernan & V. Petrosian, *Astrophys. J.* 359 (1990) 541.
- [13] S.R. Kane et al., *Astrophys. J.* 500 (1998) 1003.
- [14] K.-I. Ohki, *Solar Physics* 7 (1969) 260.
- [15] J. Kasparova et al., *Astron. Astrophys.* 466 (2013) 705.
- [16] E.C. Dickson & E.P. Kontar, *Solar Phys.* 248 (2013) 405.
- [17] M.L. McConnell et al., *Adv. Spa. Res.* 34 (2004) 462.
- [18] A. Meuris et al. *Nucl. Instrum. Meth. A* 695 (2012) 288.
- [19] C. David et al., *Microel. Engin.* 84 (2007) 1172.